Examining Tornadic Thunderstorms Through GOES-16 1-Minute Resolution Imagery

Undergraduate Research Thesis

Presented in partial fulfillment of the requirements for graduation *with honors research distinction* in Atmospheric Sciences in the undergraduate colleges of The Ohio State University

By

Edward C. Wolff IV

The Ohio State University
April 2021

Project Advisor: Professor Steven Quiring, Department of Geography

Thesis Committee: Professor Jeffery Rogers and Professor Michael Durand

TABLE OF CONTENTS

LIST OF TABLES

TABLE PAGE

LIST OF FIGURES

ABSTRACT

Since the first GOES-R (Geostationary Operational Environmental Satellite-R Series) satellite became operational in 2017, scientists and forecasters have had access to an unprecedented volume of real-time weather data, including 1-minute high resolution satellite imagery across 16 bands. Numerous studies detailing its usefulness, particularly in regards to severe weather forecasting, have been published in the years since its launch. The goal of this study is to analyze the relationship between storm characteristics as seen from satellite and a tornado's strength. Using six tornadic events, including three tornadoes from the April 12, 2020 tornado outbreak across southern Mississippi, as case studies, this project aims to build off of prior research by demonstrating the breadth of information that can be gleaned from the GOES-16 dataset. Specifically, features such as overshooting top width and cloud-top temperature associated with tornadic storms that formed are identified and analyzed. These variables are then compared to data on estimated tornado strength obtained from National Weather Service (NWS) storm surveys to attempt to define a linear relationship which could be used to predict tornadic intensity. Analysis of cloud-top temperatures (CTs) of the three tornadic storms on April 12, 2020 showed significant drops either immediately preceding or following tornadogenesis with CTs of 197 K or lower for both EF-4 storms and near 199 K for the EF-3 storm. Similarly, there was a noticeable negative correlation between overshooting top width and CT temperature with increases in OT width immediately following the strengthening of the Bassfield EF-4 tornado. This analysis demonstrates that high resolution data from GOES-16 have the potential to greatly improve nowcasting during severe weather events.

I. INTRODUCTION

In 2016, NOAA launched the first of the GOES-R (Geostationary Operational Environmental Satellite-R Series) satellites, capable of producing an unprecedented volume of real-time weather data. This includes 5-minute resolution full disk scans and 1-minute resolution imagery across all 16 spectral bands for two mesoscale sectors; five times the temporal resolution of past GOES satellites (Line et al. 2015). In addition to temporal improvements, the satellite's Advanced Baseline Imager (ABI) also improves spatial resolution by up to four times with the greatest increases coming to visible bands.

The wealth of data from these new satellites are already being integrated into the forecasting and warning processes by meteorologists across the country. One especially crucial application of these new data is in the issuance of tornado warnings. In the United States, tornadoes resulted in 76 fatalities in 2020, the highest number of deaths since 2011 when 553 people lost their lives. Additionally, in 2020, convective storms as a whole resulted in around $36 billion in property damage (Insurance Information Institute 2021). Since the 1990s, the probability of detection (POD) of tornadoes has seen a noticeable increase, resulting in more tornadoes being warned before causing damage; however, average lead time for tornado warnings (the time between a warning being issued and a tornado occurring) has remained stagnant during this time period, averaging between 15 and 20 minutes from 1990 through 2015 (Brooks & Correia 2018).

The need for timely and accurate warnings is especially great in the southeastern United States where numerous studies have indicated an increased vulnerability to tornadoes due to an increasing built environment as well as a variety of socioeconomic factors (Ashley & Strader 2016). This includes a high percentage of prefabricated homes which are especially vulnerable to

damage. In fact, Walker & Ashley (2016) also show that although the highest number of tornadoes with greater than EF1 intensity occur in the central plains, a disproportionate number of tornado fatalities occur in the Southeast. For this reason, the southeastern US has been the focus of numerous research campaigns in the past few years, most notably the VORTEX-SE project.

One issue observed both in the Southeast and across other parts of the country is the problem of gaps in radar coverage. Doppler radar plays a critical role in the warning decision process, but is traditionally believed to provide the most valuable information when the beam is below 6,000 feet since higher elevations may only scan above important low-level features (such as ground-level circulations). Unfortunately, due to geography, budgetary constraints, and a variety of other factors, there are some regions where there is no radar coverage from the NEXRAD network at these lowest elevations (NOAA, 2019). Thankfully, other observation platforms, such as satellite, can help augment the data available from radar, especially with the enhanced temporal time scales brought about by GOES-R. In regions where radar coverage is of a low quality or nonexistent, these data can be invaluable, particularly during severe weather operations. NOAA's recent report on gaps in radar coverage in the United States specifically mentions GOES-R as an alternative source of data that forecasters should utilize in addition to radar, noting that continued research will be needed to identify potentially useful products.

The goal of this study is to analyze the relationship between storm characteristics as seen from satellite and a tornado's strength. In order to categorize tornadoes by intensity, meteorologists generally rely on the Enhanced Fujita (EF) Scale, originally developed by Dr. T. Theodore Fujita in 1971 as the Fujita Scale and updated by the meteorological community in 2006 in order to better account for the quality of construction of damaged buildings surveyed

(McDonald et al. 2006). The scale relies on a series of damage indicators which allow surveyors to *estimate* tornadic wind speeds, specifically 3 second wind gusts, since direct measurements of ground-level winds rarely exist.

EF Rating	EF 0	EF 1	EF 2	EF 3	EF 4	EF 5
3 second wind gust	65-85 mph	86-110 mph	111-135 mph	136-165 mph	166-200 mph	200 + mph

Table 1: Enhanced Fujita Scale showing the range of estimated 3 second wind gusts corresponding to each category (Source: NOAA NWS SPC)

In recent years, studies have attempted to define a relationship between various remote sensing variables, such as dual polarization radar correlation coefficient, and the EF scale. These studies rely on the height of a tornadic debris signature (TDS) as measured by radar to estimate the strength of the tornadic winds at the surface (Banghoff 2015). In general, this method provides a single value, the maximum tornado intensity to have occurred during the storm's lifetime; by contrast, this study attempts to use remotely sensed data to provide a minute-by-minute estimate of tornadic intensity.

Past studies have also examined how characteristics of a storm's mesocyclone, including features visible from satellites, may relate to tornado intensity. For example, Trapp et al. (2017) examined the relationship between updraft width and tornado intensity, exploring through a numerical modeling approach whether wide mesocyclones spawn larger and more intense tornadoes at the ground. This study was followed by another which took a more observational approach, using radar data to test these theories and determining that there is a relationship

between pre-tornadic mesocyclone width and the intensity of subsequent tornadoes (Sessa & Trapp 2019).

As mentioned previously, characteristics of a storm's mesocyclone are also visible from satellite observation platforms. For example, the spatial area of a storm's overshooting top can be used to infer the width of the corresponding mesocyclone and thus, per the previously discussed studies, the strength of any tornadoes that may form. Marion et al. (2019) investigated this relationship, determining that, for their dataset from 2017 to 2019, there existed a strong correlation of R^2=0.54. They did, however, note that the observed relationship was much stronger for supercellular storms than for quasilinear convective systems (QLCS). QLCS storms occur most often in the central US during the late spring and early summer, but are also common in the Southeast, the region of interest for this paper, throughout the entire year (Ashley et al. 2019). One important caveat of both the previous studies and this current paper is that the tornadic strength estimates generated are contingent upon the formation of a tornado and do not inherently predict whether this will occur (Sessa & Trapp 2019; Marion et al. 2019).

In this study, we specifically analyze the cloud-top temperatures of the overshooting tops associated with tornadic thunderstorms. We also attempt to define a linear relationship between these values and the estimated wind speeds of the ongoing tornado on a one-minute time scale with the goal of producing a dataset that can assist forecasters in approximating the severity of an ongoing tornadic event.

II. DATA AND METHODS

Initially, tornadoes were chosen based upon four basic criteria. First, that the tornadic event occurred in the southeastern United States, as that is the main focus of this project. Second,

that the event occurred during the daytime hours, thus allowing for both visible and infrared data to be analyzed. Third, that the event resulted in at least one tornado rated as EF-3 or greater. And lastly, that the event occurred after the GOES-16 satellite became operational (that is, after 2017). Based upon these criteria, four events were selected, from which a combined six individual tornadoes were analyzed. Of these tornadoes, three were rated as EF-4, two were rated as EF-3, and one was rated as EF-2.

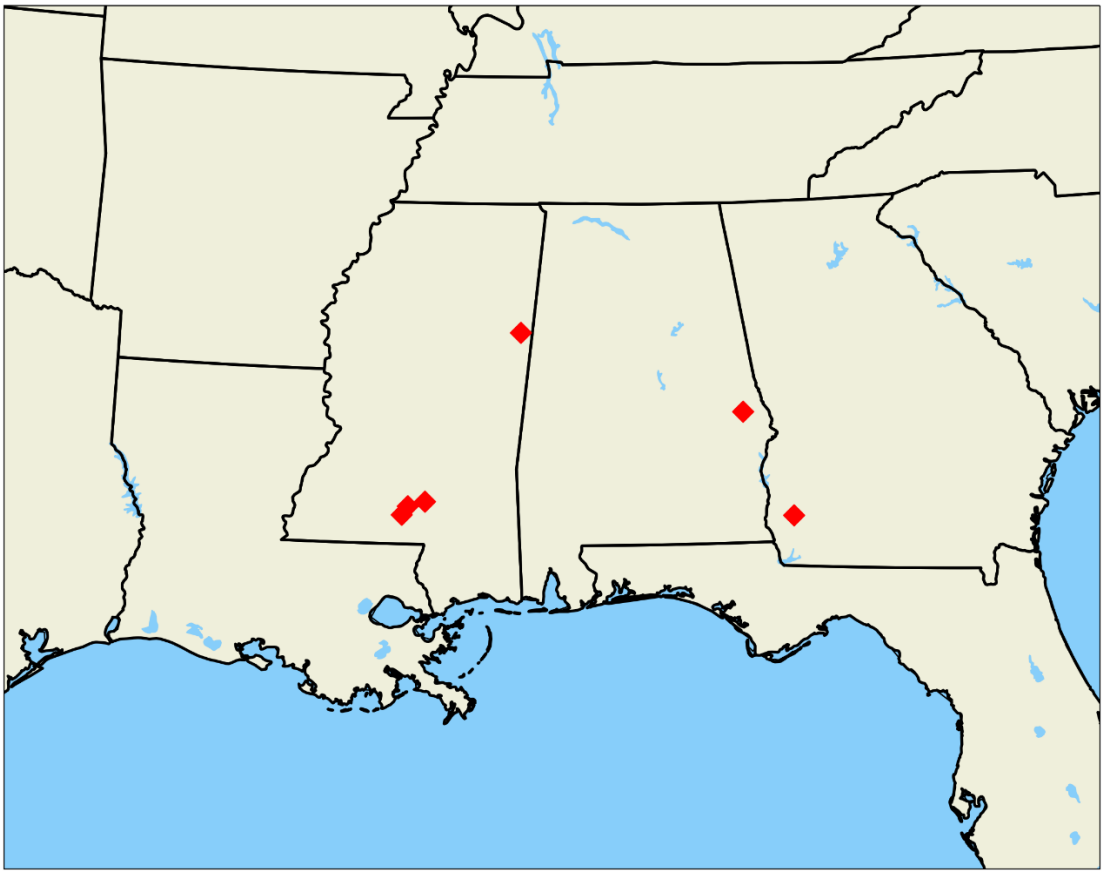

Figure 1: Map showing the approximate locations of the tornadic storms analyzed in this study

II.i SATELLITE DATA

Satellite data for this project were retrieved from the NOAA Comprehensive Large Array-Data Stewardship System (CLASS) website for each of the selected events. Both Band 2

(Visible-Red) and Band 13 (Clean Infrared) data were downloaded for the GOES-16 Mesoscale Sector positioned over the region of interest. This allowed for the retrieval of 1-minute resolution data from both bands. For the first event analyzed, April 12, 2020, satellite data were imported into MCIDAS-X where variables such as cloud-top temperature were calculated from the infrared dataset using the data probe tool. An analysis of the overshooting top width for one tornadic storm was achieved through the collection of individual latitude-longitude points which were then converted into distances using an online NOAA conversion tool. Analysis of the overshooting top width for the remaining storms was not feasible due to the "messy" nature of the convection, as is common in the Southeast. All subsequent events were analyzed in Jupyter Lab using a simple Python script (Figure 2). Using the first infrared frame to show a cold anomaly associated with an overshooting top, a latitude and longitude were calculated for the location of the storm. After inputting this coordinate into the script, a box was generated around this point and the program calculated the minimum temperature value within this box for subsequent frames. Dimensions of the defined box varied from case-to-case in order to generate the largest box possible while still only analyzing one updraft. Due to the motion of theses convective cells, this process had to be repeated several times over each storm's lifetime in order ensure that the storm's overshooting top remained within the analysis area. Since GOES-16's Mesoscale Sector was used, these values were recorded on a 1-minute timescale.

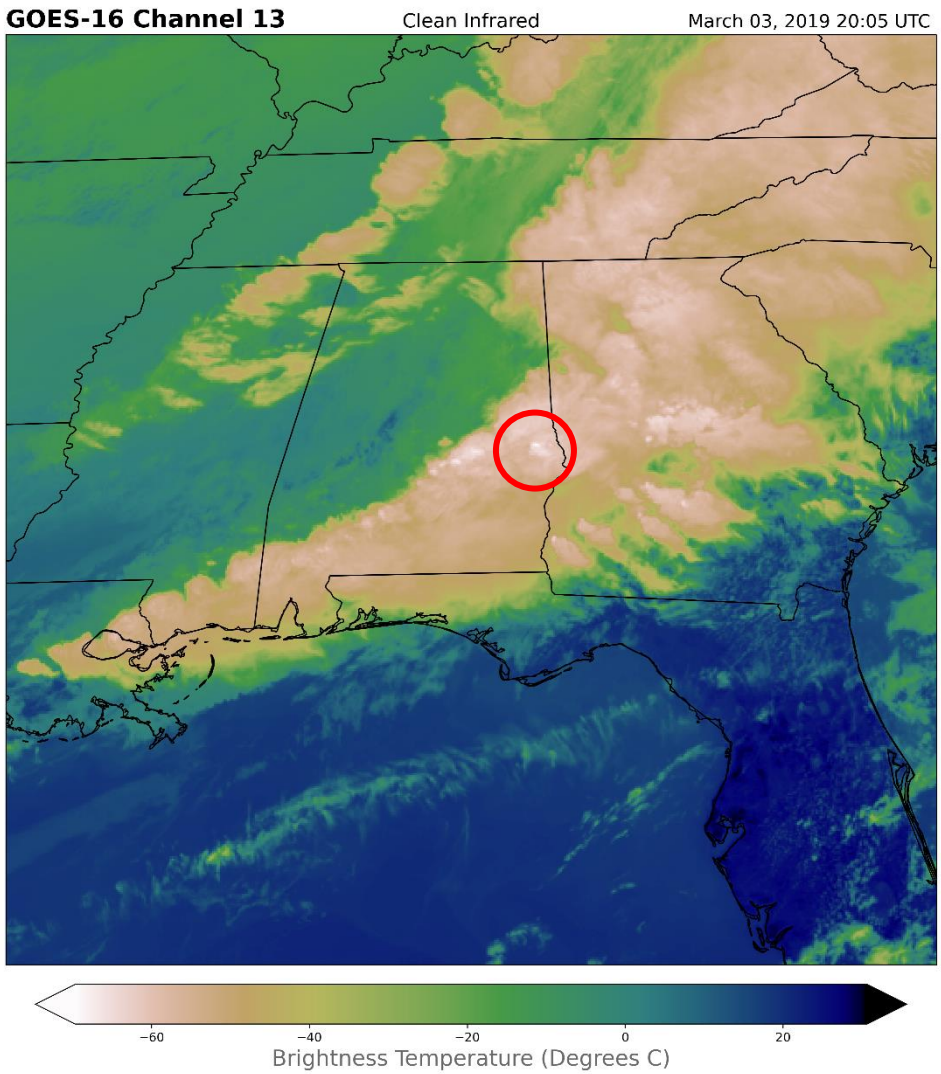

Figure 2: Satellite image from the March 3, 2019 Lee County EF-4 tornado with the associated overshooting top highlighted by the red circle

II.ii TORNADO INTENSITY DATA

The need to accurately compare these data to the relative strength of the tornado at any given time necessitated tornado strength data of similar temporal scale; unfortunately, such a dataset does not exist. The National Weather Service does however make detailed results of tornado damage surveys available through the Damage Assessment Toolkit. Each damage point is assigned an EF value corresponding to the severity of the damage at that particular location.

For some surveys, these points are also assigned an estimated time of occurrence, allowing for an estimate of the tornado's strength to be plotted over time. For instances when multiple damage points were assigned the same time, the highest EF value was used in the analysis. Due to the sporadic distribution of damage points along a storm's path, there were also time periods in which no EF values could be obtained. In these cases, the strength was estimated based upon the nearest data points.

For several of the events analyzed, an estimated time of damage was not included in the Toolkit. In these cases, radar data were used to assist with an estimation. For each storm, the nearest NEXRAD site was determined and radar data were downloaded through the National Centers for Environmental Information (NCEI) website, then displayed using Gibson Ridge GRLevel3 software. Specifically, base velocity data were utilized to identify the location of the strongest rotation at a given time. This was then compared to the data points in the Damage Assessment Toolkit to obtain an estimation of the EF strength of the storm at a given time. As with the data points described above, gaps in damage points were interpolated using the nearest available value. Likewise, gaps between radar scans also necessitated an estimation of the storm's location during some time periods.

III. RESULTS

III.i OT WIDTH AND CT TEMPERATURE

As mentioned above, the cloud-top temperature of the overshooting tops was chosen as a variable of interest after attempts to analyze overshooting top width proved unsuccessful. Using the limited dataset from the Bassfield EF-4 tornado however, we can see what appears to be a weak correlation between the cloud-top temperature and the width of the overshooting tops

(Figure 3). However, when we plot a timeseries of both OT width and CT temperature, we can see a more discernable pattern.

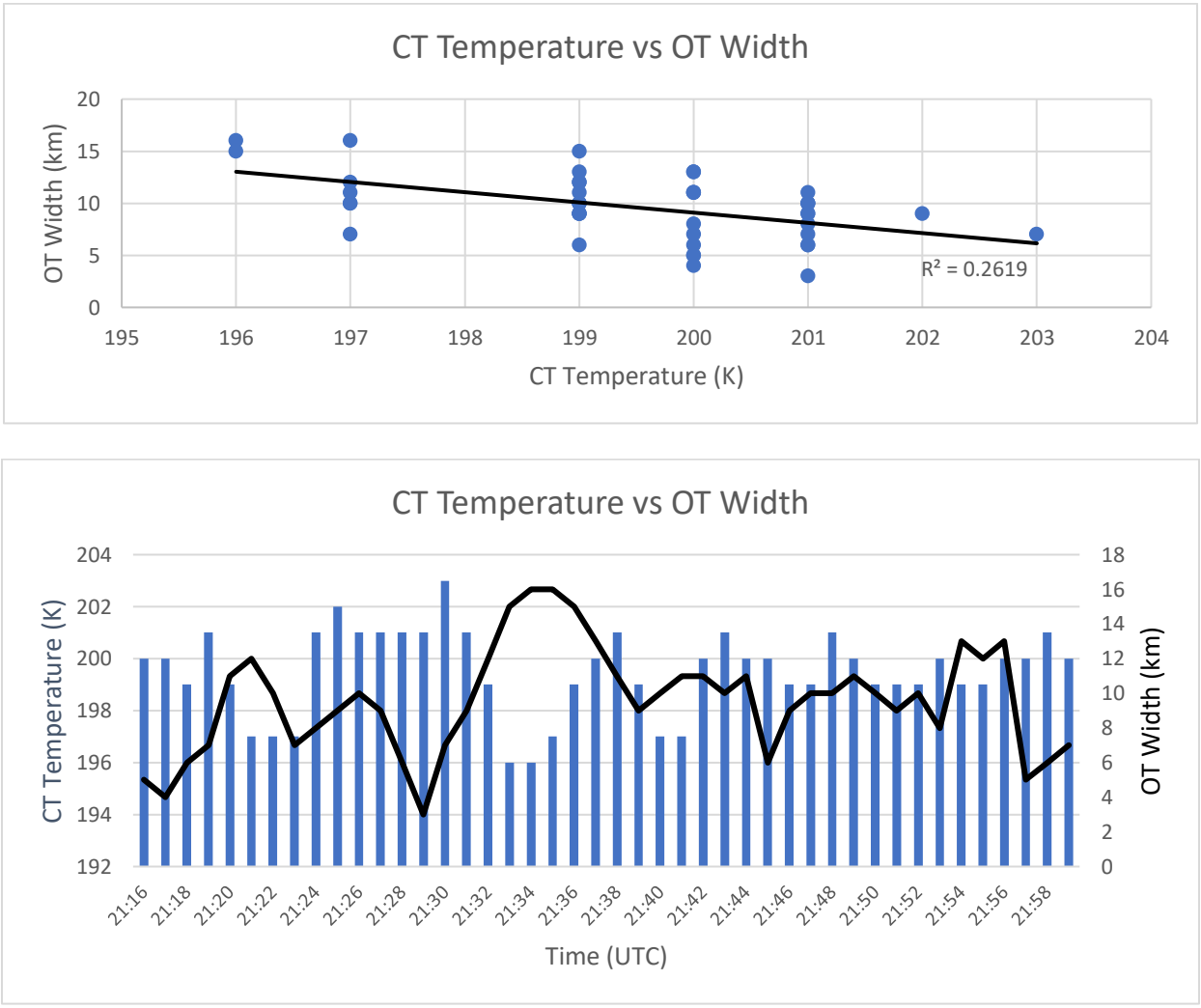

Figure 3: (Top) Relationship between CT temperature and OT width for the Bassfield, MS tornado on April 12, 2020 using data from 21:16 – 21:59 UTC. (Bottom) Time series of both CT temperature (blue bars) and OT width (black line) for the same period of the Bassfield tornado

One important detail that becomes clear in the second graph is the temporal relationship between peaks in OT width and dips in CT temperature. This is especially apparent around 21:20

UTC and 21:32 UTC where large spikes in OT width are recorded. This seems to indicate that, at least in some cases, we should be able to examine the changes in CT temperature and discern a relationship to tornado strength similar to that which we see with OT width. It is also important to note that outside of the large peaks in OT width, the relationship to CT temperature is not as apparent, with dips in OT width not always directly correlated to CT temperature spikes. This likely explains why the R^2 value remains relatively low even with a visible pattern between the two variables.

III.ii WALTHALL EF-4 TORNADO

The first of the three analyzed storms from the April 12, 2020 Outbreak to develop was the Walthall EF-4 tornado (Figure 4). This storm formed at 20:39 UTC in south-central Mississippi before moving northeastward and destroying numerous homes, resulting in four fatalities. The maximum wind speed was estimated to be near 170 mph based upon damage to a home that was completely removed from its slab.

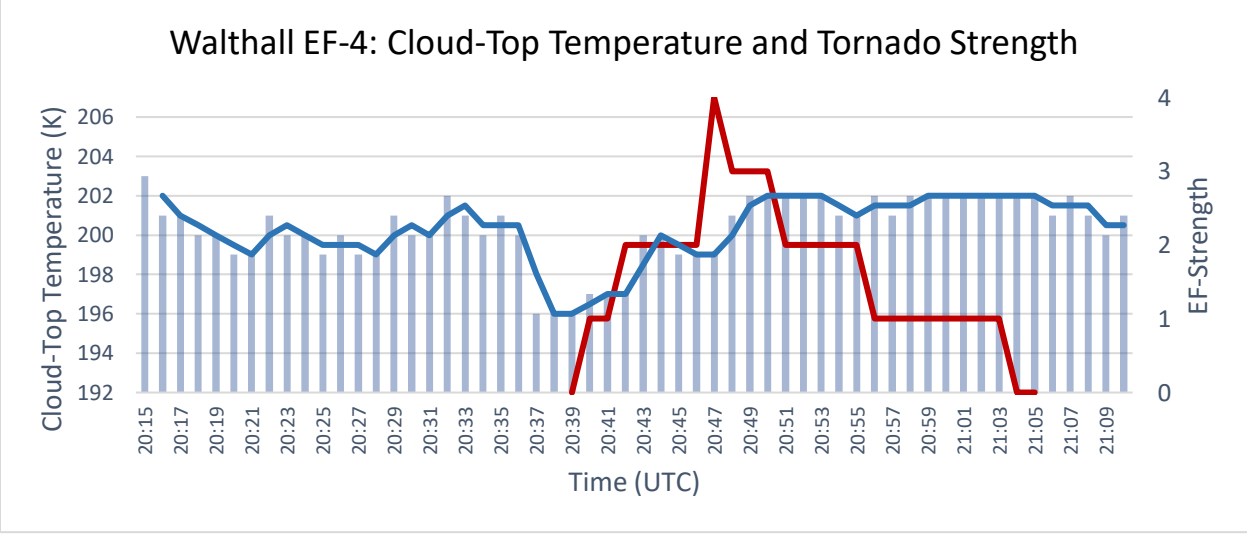

Figure 4: Time series showing CT temperature (blue bars) and tornado strength (red line) for the Walthall EF-4 tornado on April 12, 2020 which lasted from 20:39 – 21:05 UTC. Note: the blue line denotes the 3-minute running average of CT temperature

With this particular storm, CT temperatures remain relatively steady preceding tornadogenesis with values between 199 and 203 Kelvin; however, immediately before tornadogenesis occurred, there was a sharp drop in CT temperature, from 200 Kelvin to 196 Kelvin in the course of exactly one minute (20:37 UTC). This sharp drop took place roughly two minutes before the tornado formed and damage was first reported. Another smaller dip in CT temperature occurred just before the tornado reached its maximum intensity, though this drop was only about 1 Kelvin and is noticeable largely because of the 3 Kelvin rise in temperature that follows. Throughout the latter half of the tornado's life, CT temperatures remain steady as the storm's strength slowly decreases.

III.iii BASSFIELD EF-4 TORNADO

Soon after the Walthall tornado weakened, another EF-4 tornado began to form, first causing damage outside of Bassfield at 21:12 UTC (Figure 5). This storm remained on the ground for over one hour with a maximum wind speed of 190 mph and a maximum width of 2.25 miles, making it the third widest tornado on record according to the National Weather Service. In total, 8 fatalities occurred as a result of this storm.

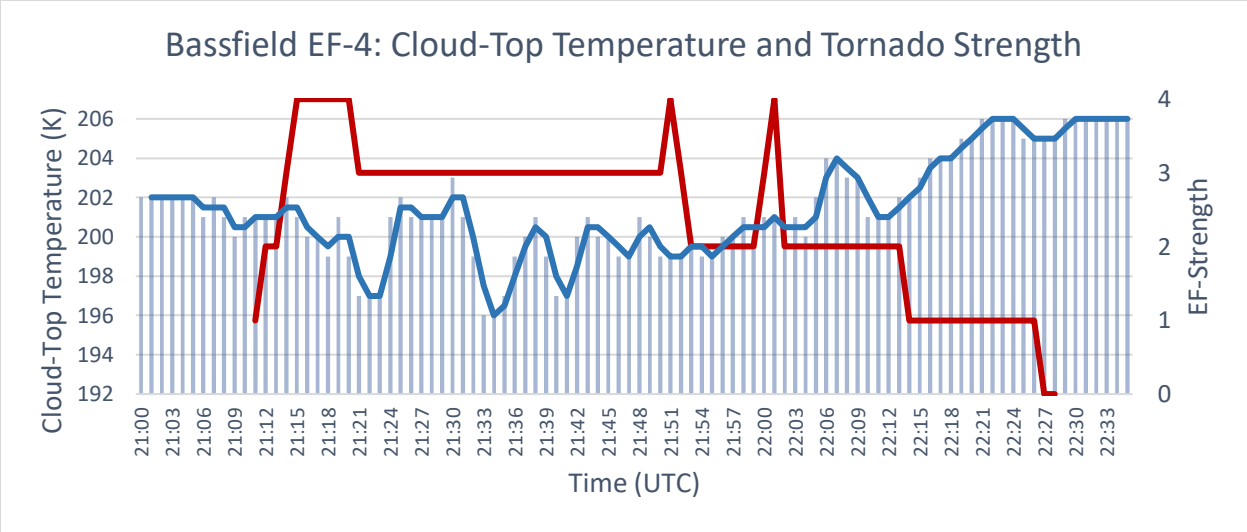

Figure 5: Time series showing CT temperature (blue bars) and tornado strength (red line) for the Bassfield EF-4 tornado on April 12, 2020 which lasted from 21:12 – 22:28 UTC. Note: the blue line denotes the 3-minute running average of CT temperature

Unlike the Walthall tornado, the Bassfield storm does not exhibit a drop in CT temperature preceding tornadogenesis. In fact, the largest drop in CT temperature occurs several minutes after the tornado had already formed and actually coincides with a temporary weakening of the tornado (from EF-4 to EF-3). Throughout this portion of the tornado's life, even though the strength of the storm appears to remain steady, the CT temperature fluctuates in a wave-like pattern with three noticeable dips occurring. This corresponds to brief, cyclic increases in overshooting top width as shown above.

III.iv OAK VALE EF-3 TORNADO

The final storm from the April 12, 2020 Outbreak to be analyzed was the Oak Vale EF-3 tornado (Figure 6). This tornado formed at 21:36 UTC while the Bassfield tornado was ongoing and produced a maximum wind speed of 150 mph. Notably, the storm's track ran nearly parallel to the two previous tornadoes, offset geographically by only a few miles to the north and temporally by around an hour.

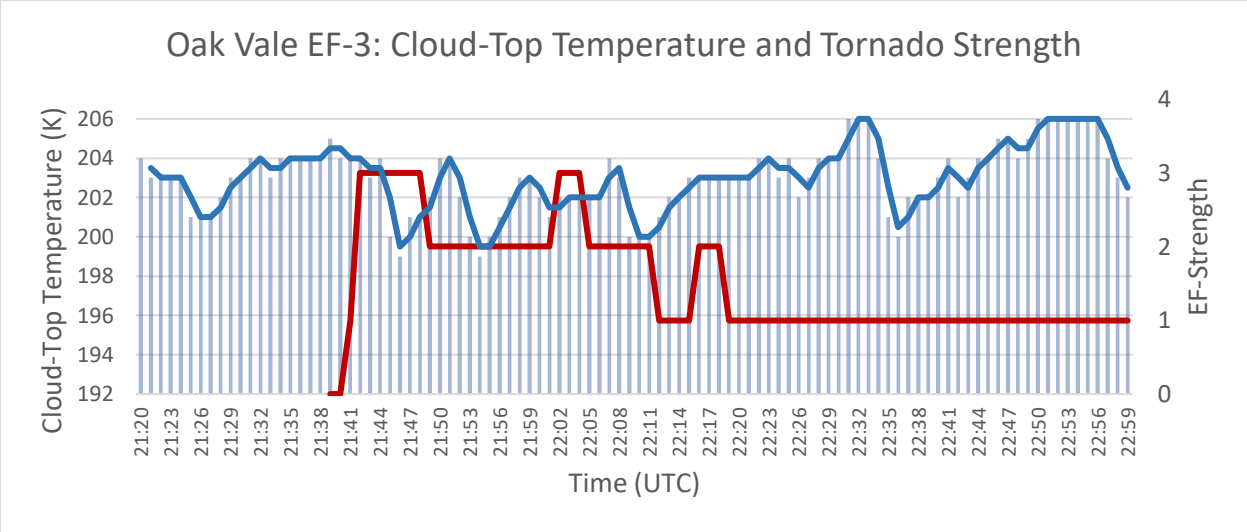

Figure 6: Time series showing CT temperature (blue bars) and tornado strength (red line) for the Oak Vale EF-3 tornado on April 12, 2020 which lasted from 21:36 – 23:07 UTC. This graph only displays data until 22:59 UTC. Note: the blue line denotes the 3-minute running average of CT temperature

Though a slight dip in CT temperature was recorded a little over ten minutes prior to the tornado forming, there was not a major temperature drop until after tornadogenesis had occurred. Similar to the Bassfield storm, the CT temperature then fluctuated in a wave-like pattern that did not directly correspond to changes in the storm's intensity. In general, the CT temperature began to rise once the storm's strength plateaued, though small dips continued to occur. It's also worth noting that the minimum temperature reached during the storm's lifetime was only 199 K compared to 196 K in both the Bassfield storm and the Walthall storm.

III.v LOWNDES COUNTY EF-3 TORNADO

Additional analysis was also performed on three other tornadic events of varying intensities. First, the Lowndes County EF-3 tornado from February 23, 2019 was examined (Figure 7). This storm touched down just south of Columbus, MS and generated an estimated maximum wind speed of 137 mph resulting in one fatality. An analysis of this storm shows a 3

Kelvin dip in CT temperature approximately four minutes before tornadogenesis with another 3 Kelvin dip as the storm reached its peak intensity. Temperatures then proceed to rise back to pre-tornado levels as the storm gradually weakens and dissipates.

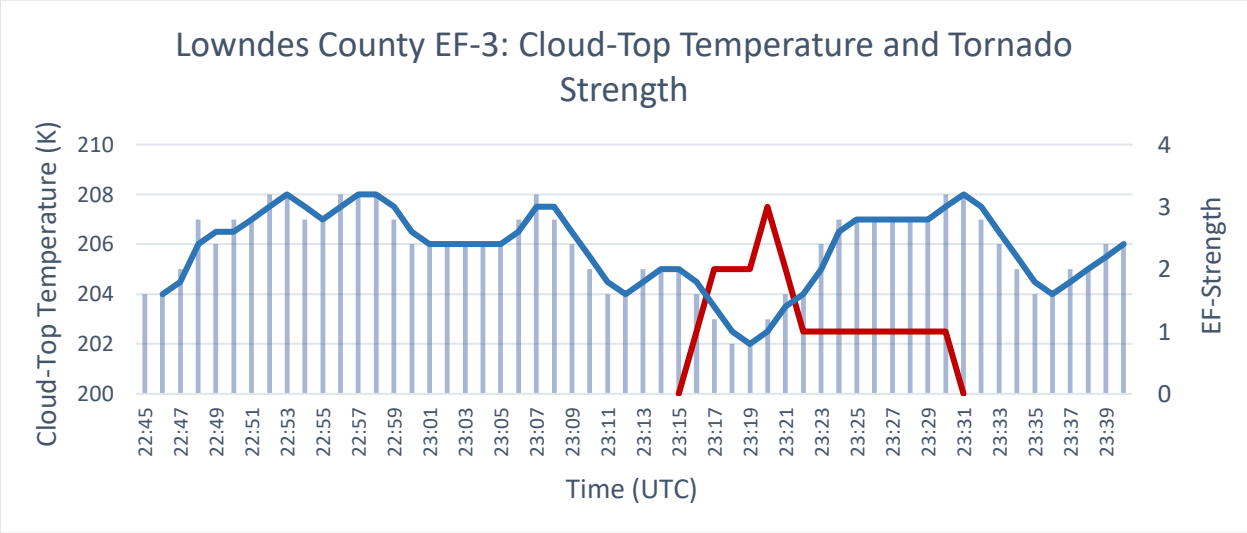

Figure 7: Time series showing CT temperature (blue bars) and tornado strength (red line) for the Lowndes County Mississippi EF-3 tornado on February 23, 2019 which lasted from 23:15 – 23:31 UTC. Note: the blue line denotes the 3-minute running average of CT temperature

III.vi LEE COUNTY EF-4 TORNADO

The second additional storm to be examined was the Lee County EF-4 tornado (Figure 8). This storm occurred on March 3, 2019 in Macon and Lee counties in Alabama, resulting in 23 fatalities and at least 90 injuries before crossing into Georgia. The maximum wind speed was estimated to be 170 mph. Similar to the previous case, a large drop in CT temperature was observed prior to tornadogenesis; in this case, a 3 Kelvin drop around 8 minutes before damage occurred. There is also a visible alignment between the rapid intensification of the tornado and the second drop in CT temperature at around 20:07 UTC. As time progresses, the link between the two variables becomes less apparent with both oscillating somewhat over time, though not always in phase.

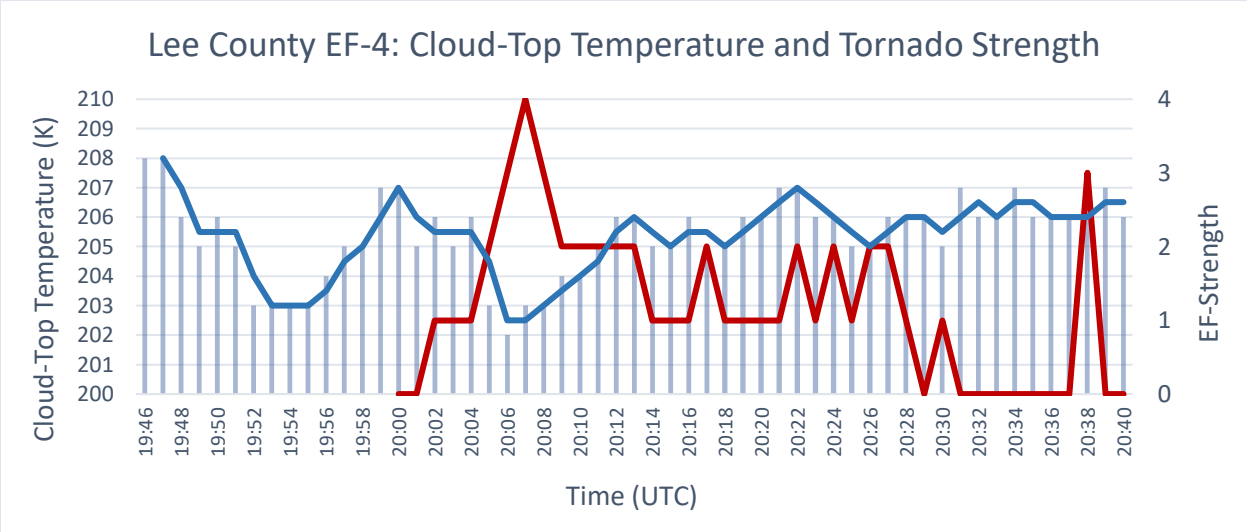

Figure 8: Time series showing CT temperature (blue bars) and tornado strength (red line) for the Lee County Alabama EF-4 tornado on March 3, 2019 which lasted from 20:00 – 21:16 UTC. This graph only displays data until 20:40 UTC when the storm crossed into Georgia. Note: the blue line denotes the 3-minute running average of CT temperature

III.vii DAMASCUS, GA EF-2 TORNADO

Lastly, one EF-2 tornado was analyzed in order to begin expanding the dataset towards lower-end tornadic events. The Damascus, GA tornado occurred on February 15, 2021 at 21:38 UTC as part of a line of severe thunderstorms moving northeastward into Georgia (Figure 9). This storm generated a maximum estimated wind speed of 130 mph, damaging several homes. There was not much of a discernable signal with this particular storm. Only a small, gradual drop in CT temperature occurred immediately prior to tornadogenesis and temperatures quickly rose as the storm weakened.

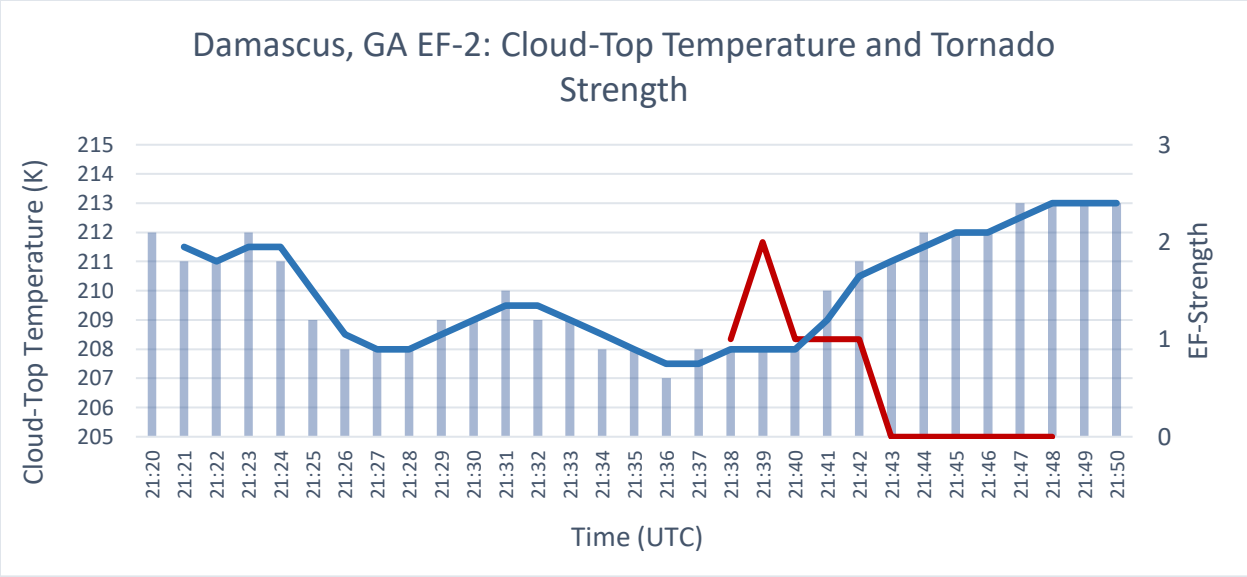

Figure 9: Time series showing CT temperature (blue bars) and tornado strength (red line) for the Damascus, Georgia EF-2 tornado on February 15, 2021 which lasted from 21:38 – 21:48 UTC. Note: the blue line denotes the 3-minute running average of CT temperature

III.viii CT TEMPERATURE AND EF RATING ANALYSIS

A direct analysis of the relationship between CT temperature and tornado intensity shows some inconsistency (Figure 10). In four of the six cases, a moderately strong relationship was visible with R^2 values above 0.4. In one of the remaining cases, the Oak Vale EF-3, a much lower R^2 was observed with a value near 0.24. And lastly, the Walthall EF-4 produced an R^2 value very close to 0. All analyzed tornadoes apart from the Walthall storm are statistically significant at alpha = 0.01. What's notable is the apparent lack of relationship between a tornado's intensity and the strength of the CT temperature/intensity relationship. Of the four cases with higher R^2 values, two were EF-4 strength, one was EF-3, and one was EF-2. Of the two lower cases, one was EF-4 strength and one was EF-3. Additionally, the storm with the lowest R^2 value, the Walthall storm, was one of the stronger tornadoes analyzed while the storm with the highest R^2 value was the Damascus EF-2, the weakest tornado analyzed.

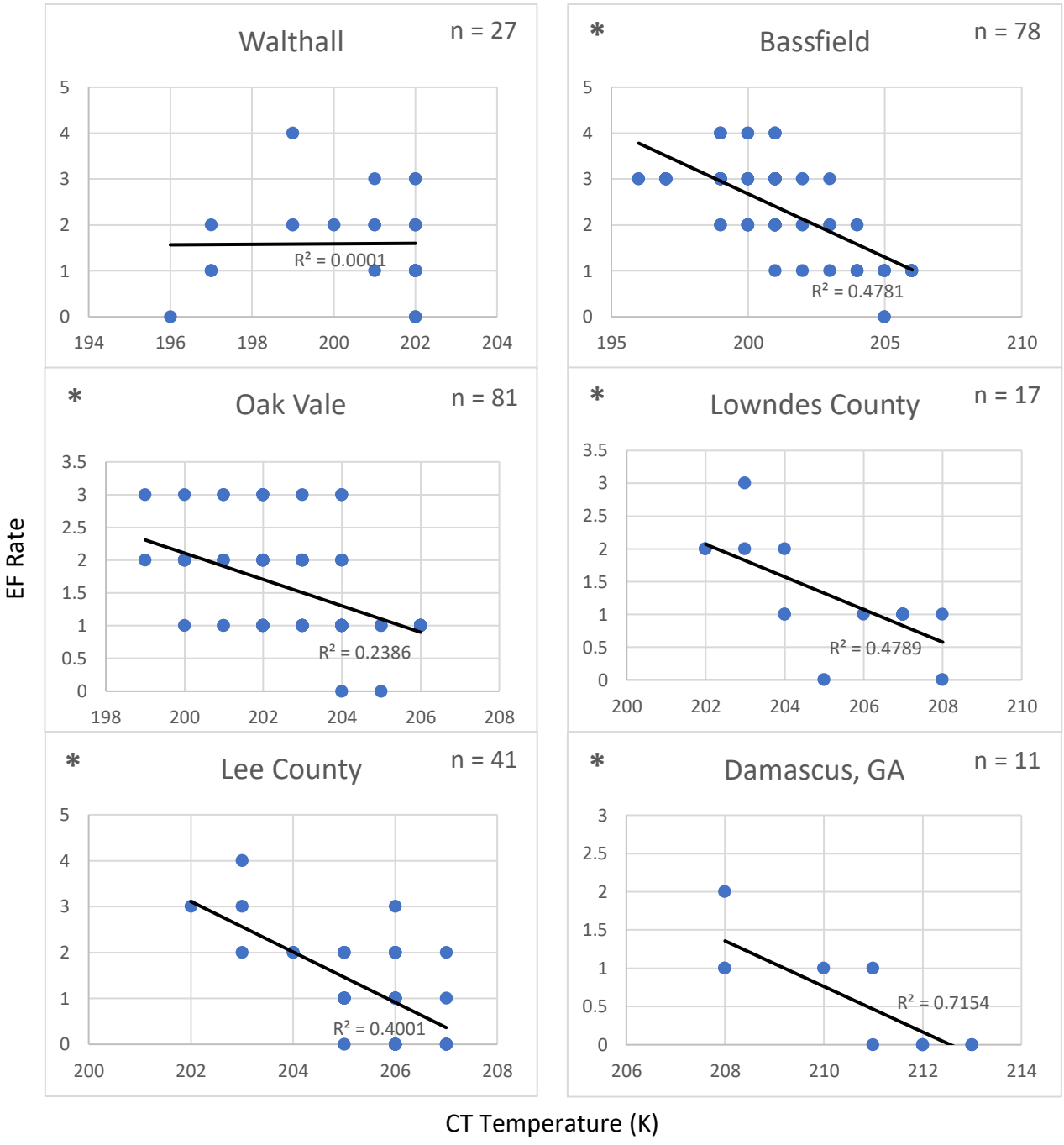

Figure 10: Comparison of coefficients of determination, representing the strength of the relationship between CT temperature and EF rating, for each of the six storms analyzed with the black line denoting the linear regression calculated for each storm (from top left to bottom right): Walthall EF-4 (4/12/20), Bassfield EF-4 (4/12/20), Oak Vale EF-3 (4/12/20), Lowndes County EF-3 (2/23/19), Lee County EF-4 (3/3/19), and Damascus, GA EF-2 (2/12/21)

*Note: * denotes statistical significance*

When data from all six storms are combined, a moderate negative correlation is visible, showing a general increase in EF rate with decreases in cloud top temperature (Figure 11). Numerous outliers are visible in this graph, including several very cool temperatures associated with low EF ratings. Many of these occurred during the April 12 storms where rapid decreases in CT temperature sometimes preceded tornadogenesis.

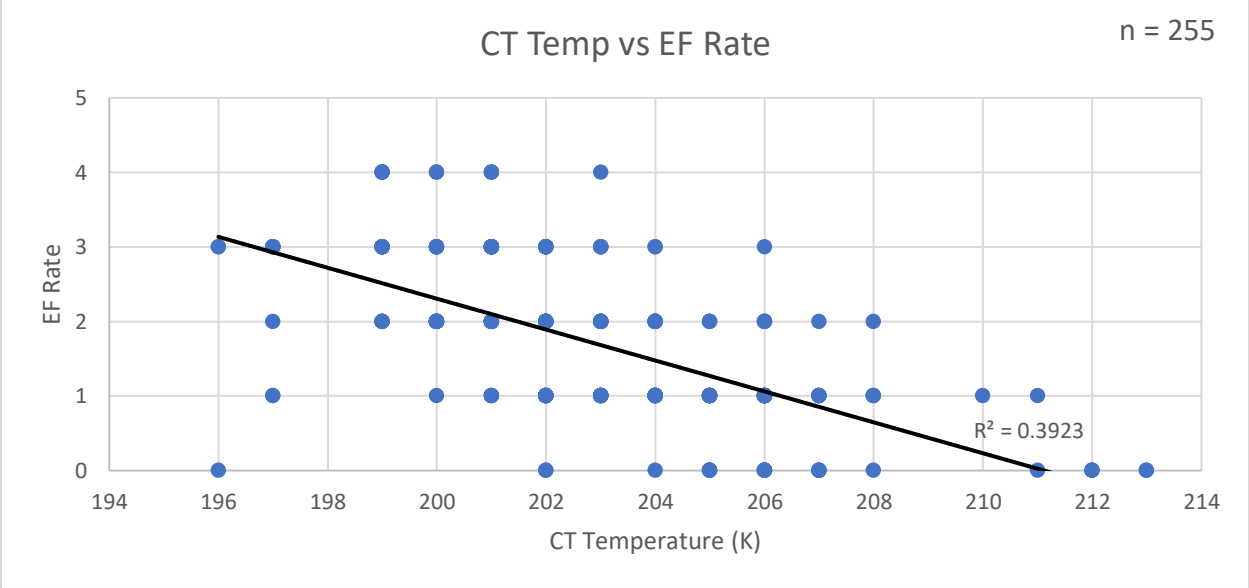

Figure 11: Linear regression analysis using all one-minute data points collected from all six tornado case studies described above. Note: the black line denotes the linear regression calculated for the entire dataset

This trend can also be visualized using a box and whisker plot, similar to analyses relating correlation coefficient debris signature height to EF strength (Banghoff 2015). In this particular chart (Figure 12), EF-3 through EF-5 values are combined due to the lack of data points for higher-end storms. This demonstrates that, given a CT temperature, the EF strength can be estimated with some degree of certainty, though there is considerable overlap between categories and several outliers.

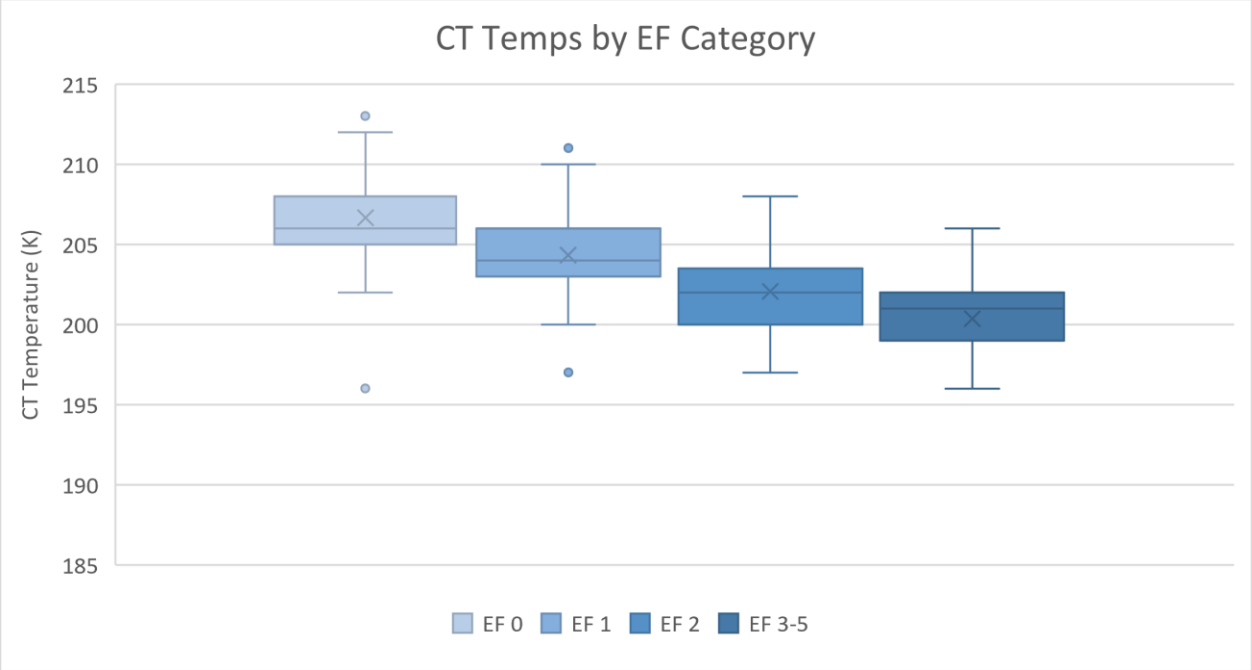

Figure 12: Analysis of CT temperatures separated by their corresponding EF rating. The EF-0 category contains 27 data points, the EF-1 category contains 98, EF-2 contains 69, and EF-3-5 contains a total of 59 data points. Note: EF-3 through EF-5 are binned together due to the relatively small number of data points within the EF-4 category (10 points) and the lack of any data points for EF-5 storms

In an attempt to remedy some of the aforementioned issues relating to the slight time differences between CT temperature drops and EF rate changes, an additional set of graphs were created using 3-minute binned data. In this analysis, both CT temperatures and EF rates were averaged over 3-minute periods and EF rates were rounded to the nearest whole number. An examination of the R^2 values for these graphs compared to those in Figure 10 shows only marginal improvements overall. In general, cases that already had higher R^2 showed larger improvements than those with very low values, such as the Walthall storm. For example, using this binning method, the Bassfield R^2 improved from 0.4781 to 0.5751 while the Walthall R^2 had

only a modest improvement from 0.0001 to 0.0153. Given that changes to the final data were only marginal, this method was not utilized in the final analysis.

IV. DISCUSSION

Overall, a moderate correlation can be seen between cloud-top temperature and tornadic strength, though the relationship is not as strong as what has been observed in previous studies relying on OT area and radar-observed mesocyclone width. The overall correlation measured in this study, using all six cases, was approximately R^2=0.39. By contrast, radar-observed mesocyclone width exhibited a correlation of R^2=0.75 (Sessa & Trapp 2019) and overshooting top area had a correlation of R^2=0.54. (Marion et al. 2019). It is worth noting that four of the six individual cases within this study did exhibit correlations closer to these values (that is, greater than 0.4) with one case having an R^2 value greater than 0.7.

One possible reason for the lower R^2 values seen in this study has to do with the time delay between changes in CT temperature and intensity. This is especially pronounced in the Walthall EF-4 tornado which showed essentially no correlation (R^2=0.0001) and where the spike in EF strength was seen just after a rapid drop in CT temperature with a time delay of ~10 minutes. Conversely, in the case of the Bassfield EF-4 tornado, the drop in CT temperature occurred *after* the tornado peaked in intensity for the first time, with a time delay of ~7 minutes. In the other cases examined, only small time delays were observed. Due to this lack of consistency, it is difficult to account for these time discrepancies within the statistical analysis.

Another likely reason for the overall lower correlation observed in this study stems from the size of the dataset. Though over 250 individual data points were examined, these correspond to only 6 individual storms, an incredibly small dataset compared to the previous studies (Sessa

& Trapp 2019; Marion et al. 2019). With the expansion of the dataset beyond the three initial storms from April 12, 2020, noticeable improvements in the cumulative correlation were observed, thus it is probable that the inclusion of additional cases would result in additional improvements, mainly by lessening the impact of cases which exhibited large time delays, assuming that these cases are outliers.

All of the results presented here do carry an important caveat. Since all cases examined were known to have produced a tornado, the resulting wind speed estimates are contingent upon the observed storm producing a tornado and do not in any way indicate whether this will occur. Thus, were these data to be used in an operational forecasting setting, it would have to be accompanied by other data sources, especially radar and mesoscale analyses, to determine whether a tornado is occurring or is likely to occur before estimating the potential intensity. This is similar to the aforementioned studies examining updraft width and overshooting top area whose results are also contingent upon tornado formation.

V. CONCLUSION

Improvements in satellite technology over the past several years have opened the door to a wide variety of possible applications, particularly in regards to severe weather operations. One minute resolution imagery from the GOES-R series in particular allows for the observation of storm evolution at a temporal scale that is even finer than most radar sites provide. This high level of detail can be especially useful for monitoring storm characteristics such as the overshooting tops which can rise and fall rapidly during a storm's lifecycle. As past studies have shown, the width of these features can be used to estimate the intensity of any tornadoes which may occur beneath the storm with a fairly high level of accuracy. Likewise, this study was able

to demonstrate a similar (though weaker) relationship between the temperature of a storm's overshooting tops and tornadic intensity using a dataset built from a small set of case studies from the Southeast. Although the correlation observed in this study was smaller than those found in previous publications, some of the individual cases did exhibit better results with over half having an R^2 value higher than 0.4.

Future research would continue to expand the dataset, including a larger number of more common low-end tornadic events and possibly expanding the scope of the study beyond the Southeast. The use of null cases could also be explored to determine if cloud-top temperature can itself predict the potential for tornadic occurrence, though current research suggests that this is unlikely as many supercells with strong updrafts and cold cloud-tops fail to produce tornadoes. Once the dataset is sufficiently expanded, it would also be possible to analyze whether the minimum observed CT temperature throughout a storm's lifetime is a strong indicator of the maximum tornadic intensity. Though this would not give forecasters the minute-by-minute information this study hoped to provide, it may help negate the effects of the time delays discussed earlier. Early results with the small set of storms in this study yielded a very promising R^2 value above 0.6, but additional case studies are needed to increase confidence. It would also be prudent for any additional research to take advantage of other statistical methods, beyond linear regression, that are perhaps better suited for categorical variables and could provide more details on data trends. Ideally, the results of this work would be used in conjunction with information on OT width, radar characteristics, and the mesoscale environment to provide a reasonable estimate of potential tornadic strength, thus increasing forecaster confidence and improving the timing and quality of tornado warnings.

VI. ACKNOWLEDGEMENTS

This research was funded by the National Science Foundation (AGS-1757892) through the 2020 REU program at the University of Alabama in Huntsville. Portions of this thesis were presented at the 2021 AMS Student Conference. The author would like to thank his mentors at UAH including Dr. John Mecikalski, David Haliczer, and Christopher Tracy for all their feedback, support, and sample code. In addition, thanks to the REU leadership team, Ryan Wade and Vanesa Martin, for their support throughout the REU program. Lastly, special thanks to Dr. Steven Quiring for his constant guidance throughout the thesis and defense process.

VII. REFERENCES

Ashley, W.S. and S.M. Strader, 2016: RECIPE FOR DISASTER: How the Dynamic Ingredients of Risk and Exposure are Changing the Tornado Disaster Landscape, *Bull. Amer. Meteor. Soc.*, **97**, 767-86, doi: 10.1175/BAMS-D-15-00150.1

Ashley, W.S., A.M. Haberlie, and J. Strohm, 2019: A Climatology of Quasi-Linear Convective Systems and Their Hazards in the United States, *Wea. Forecasting*, **34**, 1605-31, doi: 10.1175/WAF-D-19-0014.1

Banghoff, J., 2015: Correlation of Tornado Intensity with Dual-Polarization Radar Information. Undergraduate Thesis, Dept. of Geography, The Ohio State University, 31 pp., https://kb.osu.edu/bitstream/handle/1811/73720/Honors_Thesis.pdf

Brooks, H.E. and J. Correia Jr., 2018: Long-Term Performance Metrics for National Weather Service Tornado Warnings, *Wea. Forecasting*, **33**, 1501-11, doi: 10.1175/WAF-D-18-0120.1

Insurance Information Institute, 2021: Facts + Statistics: Tornadoes and thunderstorms. Accessed 10 April 2021, https://www.iii.org/fact-statistic/facts-statistics-tornadoes-and-thunderstorms

Line, W.E., T.J. Schmit, D.T. Lindsey, and S.J. Goodman, 2015: Use of Geostationary Super Rapid Scan Satellite Imagery by the Storm Prediction Center, *Wea. Forecasting*, **31**, 483-94, doi: 10.1175/WAF-D-15-0135.1

Marion, G.R., R.J. Trapp, and S.W. Nesbitt, 2019: Using Overshooting Top Area to Discriminate Potential for Large, Intense Tornadoes, *Geophysical Research Letters*, **46**, 12520-26, doi: 10.1029/2019GL084099

McDonald, J. and Coauthors, 2006: A Recommendation for an Enhanced Fujita Scale (EF Scale), 111 pp., https://www.depts.ttu.edu/nwi/Pubs/FScale/EFScale.pdf

NOAA, 2019: Report to Congress: Gaps in NEXRAD Radar Coverage, 28 pp.

Sessa, M.F. and R.J. Trapp, 2019: Observed Relationship between Tornado Intensity and Pretornadic Mesocyclone Characteristics, *Wea. Forecasting*, **35**, 1243-61, doi: 10.1175/WAF-D-19-0099.1

Trapp, R.J., G.R. Marion, and S.W. Nesbitt, 2017: The Regulation of Tornado Intensity by Updraft Width, *J. Atmos. Sci.*, **74**, 4199-211, doi: 10.1175/JAS-D-16-0331.1\